

NUMERICAL SCHUBERT CALCULUS VIA THE LITTLEWOOD-RICHARDSON HOMOTOPY ALGORITHM

ANTON LEYKIN, ABRAHAM MARTÍN DEL CAMPO, FRANK SOTTILE, RAVI VAKIL,
AND JAN VERSCHELDE

ABSTRACT. We give a detailed description of the Littlewood-Richardson homotopy algorithm, which uses numerical continuation to compute solutions of Schubert problems on Grassmannians and is based on the geometric Littlewood-Richardson rule. In addition to providing algorithmic details of the geometric Littlewood-Richardson rule, we discuss mathematical aspects of the algorithm, including an efficient formulation of Schubert problems in local Stiefel coordinates as systems of equations.

The Schubert calculus on the Grassmannian [20] involves problems of determining the linear subspaces that have specified positions with fixed flags of linear spaces. This is a rich class of well-understood geometric problems that appear in applications, such as the output pole placement problem in linear systems theory [3, 2, 4, 5, 6, 25, 26, 39], and this class serves as a laboratory for investigating new phenomena in enumerative geometry, such as reality [8, 12, 13, 15, 24, 27, 30, 31, 32] or Galois groups [22, 24, 34]. While classical algorithms count the numbers of solutions [7], these applications drive a need to compute the actual solutions to Schubert problems.

Numerical algebraic geometry gives methods, based on numerical homotopy continuation, to compute approximations to solutions of systems of polynomial equations. The sophisticated general methods currently in use are inefficient for solving Schubert problems, and *numerical Schubert calculus* consists of numerical algorithms adapted to the structure of Schubert problems. A homotopy algorithm is *optimal* if no solution path diverges for generic instances of the problem. The first such optimal algorithm for Schubert calculus was the Pieri homotopy algorithm for solving special Schubert problems [16]—these are Schubert problems where each condition is that the linear subspace simply meets a fixed subspace. That algorithm is based on a proof of Pieri’s rule using geometric specializations [29]. It was implemented and refined [18, 23, 38, 39, 40], and has been used to compute Galois groups of Schubert problems [22].

The more general Littlewood-Richardson rule was given a proof using geometric specializations organized by a combinatorial checkers game [35, 36]. As with the geometric Pieri rule, this leads to a homotopy algorithm that may be used to compute solutions to all Schubert problems on Grassmannians. This algorithm was sketched in [33]. Our primary purpose is to describe this Littlewood-Richardson homotopy algorithm in full.

2010 *Mathematics Subject Classification.* 14N15, 65H10.

The authors thank the American Institute of Mathematics for supporting the project through their SQuaREs program.

Work of Sottile supported in part by the National Science Foundation under grant DMS-1501370.

This algorithm, both in its details and overall structure, is the most complicated homotopy algorithm of which we are aware. This includes the Bézout, multihomogeneous, polyhedral [17], cheater/parameter, and regeneration [11].

We also explain a new, efficient way to generate local equations for Schubert varieties. The Littlewood-Richardson homotopy algorithm has been implemented both in Macaulay2 [9] and in PHCPack [37], and we give some information on its performance. A future publication will give implementation details.

Section 1 gives background on the Schubert calculus and numerical homotopy continuation. Section 2 is the heart of the paper, for it describes the Littlewood-Richardson homotopy algorithm in detail.

- (1) Mathematical details of the implementation
- (2) What can we compute

1. SCHUBERT CALCULUS AND HOMOTOPY CONTINUATION

We describe Schubert problems and explain how they may be represented on a computer, give an efficient set of equations for Schubert problems, and discuss numerical homotopy continuation.

1.1. Schubert problems. The *Grassmannian* $\text{Gr}(k, n)$ of k -planes in \mathbb{C}^n is a complex manifold of dimension $k(n-k)$ that is naturally an algebraic subvariety of Plücker space $\mathbb{P}^{\binom{n}{k}-1} = \mathbb{P}(\wedge^k \mathbb{C}^n)$. Plücker space has coordinates p_α indexed by *brackets*, which are k -element subsets of $[n] := \{1, \dots, n\}$, written in increasing order $\alpha: \alpha_1 < \dots < \alpha_k$. Write $\binom{[n]}{k}$ for this set of brackets.

A *flag* F is an increasing sequence of linear subspaces,

$$F : F_1 \subset F_2 \subset \dots \subset F_n = \mathbb{C}^n, \quad \text{with} \quad \dim F_i = i.$$

A bracket $\alpha \in \binom{[n]}{k}$ and a flag F determine a *Schubert variety*,

$$X_\alpha F := \{H \in \text{Gr}(k, n) \mid \dim(H \cap F_{\alpha_i}) \geq i \text{ for } i = 1, \dots, k\}.$$

This consists of all k -planes H having *position* α with respect to the flag F . The Schubert variety $X_\alpha F$ has codimension $\|\alpha\| := k(n-k) - \sum_i (\alpha_i - i)$ in $\text{Gr}(k, n)$.

The geometric problems studied in Schubert calculus are given by lists of brackets $(\alpha^1, \dots, \alpha^s)$ and flags F^1, \dots, F^s , and involve understanding the set of k -planes having position α^j with respect to flag F^j for each $j = 1, \dots, s$. This set is the intersection

$$X_{\alpha^1} F^1 \cap X_{\alpha^2} F^2 \cap \dots \cap X_{\alpha^s} F^s. \tag{1}$$

When the flags F^1, \dots, F^s are general and we have $\|\alpha^1\| + \dots + \|\alpha^s\| = k(n-k)$, this intersection is zero-dimensional and transverse [19] and its number, $d(\alpha^1, \dots, \alpha^s)$, of points does not depend on the flags. This number may be computed using combinatorial algorithms from the Schubert calculus [7]. Because of this, we call a list of brackets $(\alpha^1, \dots, \alpha^s)$ satisfying $\|\alpha^1\| + \dots + \|\alpha^s\| = k(n-k)$ a *Schubert problem*. An *instance* of that Schubert problem is given by flags F^1, \dots, F^s , and its *solutions* are the points of the intersection (1).

The most basic Schubert problem is $X_\alpha F \cap X_\beta M$ with $\|\alpha\| + \|\beta\| = k(n-k)$. It has no solutions unless $\alpha_i + \beta_{k+1-i} = n+1$ for $i = 1, \dots, k$, and in that case it is the singleton,

$$X_\alpha F \cap X_\beta M = \left\{ \bigoplus_{i=1}^k F_{\alpha_i} \cap M_{\beta_{k+1-i}} \right\}, \quad (2)$$

where the flags F and M are in general position, so that $F_{\alpha_i} \cap M_{\beta_{k+1-i}}$ is one-dimensional.

1.2. Representing Schubert problems on a computer. To solve a Schubert problem on a computer requires that the problem be formulated as a system of polynomial equations in some coordinates. There are several available formulations, including global Pücker coordinates, local Stiefel coordinates, and more exotic primal-dual [10] or lifted [14] coordinates. Local Stiefel coordinates involve the fewest variables.

We represent elements of \mathbb{C}^n as column vectors whose rows correspond to the standard ordered basis $\mathbf{e}_1, \dots, \mathbf{e}_n$ of \mathbb{C}^n . An ordered basis $\mathbf{f}_1, \dots, \mathbf{f}_n$ of \mathbb{C}^n forms the columns of an invertible matrix F and vice-versa with the standard basis corresponding to the identity matrix, I . Given such a basis/matrix, we obtain a flag whose i -dimensional subspace is the span of $\mathbf{f}_1, \dots, \mathbf{f}_i$. Matrices F, F' give the same flag if and only if there is an invertible upper triangular matrix T with $F' = FT$. We allow a mild ambiguity and use the same symbol for an invertible matrix and the corresponding flag.

The *Stiefel manifold* is the set $\mathcal{M}_{n \times k}$ of $n \times k$ matrices of full rank k . Taking column space gives a map $\phi: \mathcal{M}_{n \times k} \rightarrow \text{Gr}(k, n)$ which is a principal $GL_k(\mathbb{C})$ -bundle. This admits a (discontinuous) section given by putting any matrix in a fiber into reverse column reduced echelon form. The set \mathcal{X}_α of echelon matrices with pivots in rows α is isomorphic to $\mathbb{C}^{k(n-k)-\|\alpha\|}$. Under ϕ , the set \mathcal{X}_α is isomorphic to a dense open subset of the Schubert variety $X_\alpha I$. For example, here are the sets \mathcal{X}_α when $n = 6$ and $k = 3$ for the sequences $\alpha = (4, 5, 6)$, $(2, 4, 6)$, and $(2, 3, 5)$, respectively, where x_{ij} is an indeterminate:

$$\begin{pmatrix} x_{11} & x_{12} & x_{13} \\ x_{21} & x_{22} & x_{23} \\ x_{31} & x_{32} & x_{33} \\ 1 & 0 & 0 \\ 0 & 1 & 0 \\ 0 & 0 & 1 \end{pmatrix} \quad \begin{pmatrix} x_{11} & x_{12} & x_{13} \\ 1 & 0 & 0 \\ 0 & x_{32} & x_{33} \\ 0 & 1 & 0 \\ 0 & 0 & x_{53} \\ 0 & 0 & 1 \end{pmatrix} \quad \begin{pmatrix} x_{11} & x_{12} & x_{13} \\ 1 & 0 & 0 \\ 0 & 1 & 0 \\ 0 & 0 & x_{43} \\ 0 & 0 & 1 \\ 0 & 0 & 0 \end{pmatrix}$$

For a subvariety Y of $\text{Gr}(k, n)$, any set $\mathcal{Y} \subset \phi^{-1}(Y)$ with $\phi: \mathcal{Y} \rightarrow Y$ birational will be called *Stiefel coordinates* for Y . In particular, the set \mathcal{X}_α gives Stiefel coordinates for the Schubert variety $X_\alpha I$. This description is equivariant in that if F is an invertible matrix/flag, then $F\mathcal{X}_\alpha$ gives Stiefel coordinates for $X_\alpha F$.

Given a point $H \in \mathcal{M}_{n,k}$, the condition that the k -plane $\phi(H)$ lies in $X_\alpha F$ may be expressed in terms of the rank of augmented matrices,

$$\text{rank} \left(H \mid F_{\alpha_i} \right) \leq k + \alpha_i - i \quad \text{for } i = 1, \dots, k. \quad (3)$$

Thus for each $i = 1, \dots, k$, all square $(k + \alpha_i - i + 1) \times (k + \alpha_i - i + 1)$ minors of the matrix $(H \mid F_{\alpha_i})$ vanish. This gives

$$\sum_{i=1}^k \binom{n}{k + \alpha_i - i + 1} \binom{k + \alpha_i}{k + \alpha_i - i + 1}$$

minors, which are polynomials in the entries of H . There are no minors when $\alpha_i = n - k + i$ and conditions i when $\alpha_i + 1 = \alpha_{i+1}$ are redundant. For example, when $k = 4$, $n = 8$, and $\alpha = (3, 4, 7, 8)$ the only condition that matters is $\dim H \cap F_4 \geq 2$ or $\text{rank}(H \mid F_4) \leq 6$, which is given by the 64 non-maximal 7×7 minors of the 8×8 matrix $(H \mid F_4)$, of which 32 are cubics and 32 are quartics in the entries of H .

This discussion shows that we may model the intersection of a subset $Y \subset \text{Gr}(k, n)$ with a collection of Schubert varieties,

$$Y \cap X_{\alpha^1} F^1 \cap X_{\alpha^2} F^2 \cap \dots \cap X_{\alpha^s} F^s,$$

by first selecting a set $\mathcal{Y} \subset \mathcal{M}_{k,n}$ of Stiefel coordinates for Y and then generating the minors implying the rank conditions (3), for each pair α^i, F^i .

1.3. Efficient representation of Schubert problems. The formulation of $X_{(3,4,7,8)} F$ in local Stiefel coordinates involved the 7×7 minors of a matrix $(H \mid F_4)$ with 32 cubics and 32 quartics. If the entries of H are indeterminates, then these span a 33-dimensional space of polynomials with 16 cubics and 17 quartics. The quartics suffice, but it is not clear *a priori* which 17 of the 32 are needed. Even if this were known, computing these 17 minors requires computing $17 \cdot \binom{7}{4} = 595$ full (4×4) minors of the 8×4 matrix H of variables—computing each of its $70 = \binom{8}{4}$ minors on average 8.5 times. A related overcomputing of the minors of F_4 also occurs. This is inefficient. We show how to compute the 17 generating quartics, and avoid overcomputing the minors of H and F_4 .

The Plücker embedding $\text{Gr}(k, n) \hookrightarrow \mathbb{P}(\wedge^k \mathbb{C}^n)$ is induced by the map $\text{Mat}_{n \times k}(\mathbb{C}) \rightarrow \wedge^k \mathbb{C}^n$ given by the $\binom{n}{k}$ maximal minors of a matrix $H \in \text{Mat}_{n \times k}(\mathbb{C})$

$$H \mapsto \left(p_{\alpha}(H) \mid \alpha \in \binom{[n]}{k} \right) \in \wedge^k \mathbb{C}^n,$$

where $p_{\alpha}(H) := \det(h_{\alpha_i, j})_{i,j=1}^k$ and $h_{i,j}$ are the entries of H . These minors $p_{\alpha}(H)$ are the *Plücker coordinates* of H . The image (which is $\text{Gr}(k, n)$) is cut out by the quadratic Plücker relations [7, §9.1, Lemma 1].

The image of the Schubert variety $X_{\alpha} I$ is cut out from the Grassmannian by a subset of Plücker coordinates. Specifically, a k -plane H lies in $X_{\alpha} I$ if and only if $p_{\beta}(H) = 0$ for all $\beta \in \binom{[n]}{k}$ with $\beta \not\leq \alpha$. This uses the partial order on the index set $\binom{[n]}{k}$ of brackets: $\alpha \leq \beta \Leftrightarrow \alpha_i \leq \beta_i$ for $i = 1, \dots, k$.

Example 1.1. When $n = 8$, $k = 4$, and $\alpha = (3, 4, 7, 8)$, there are 17 indices β with $\beta \not\leq \alpha$,

$$\begin{aligned} & (5, 6, 7, 8), (4, 6, 7, 8), (3, 6, 7, 8), (4, 5, 7, 8), (2, 6, 7, 8), (3, 5, 7, 8), (4, 5, 6, 8), \\ & (1, 6, 7, 8), (2, 5, 7, 8), (3, 5, 7, 8), (4, 5, 6, 7), (1, 5, 7, 8), (2, 5, 6, 8), (3, 5, 6, 7), \\ & (1, 5, 6, 7), (2, 5, 6, 7), (1, 5, 6, 7). \end{aligned}$$

◇

Observe that $H \in X_\alpha F$ if and only if $F^{-1}H \in X_\alpha I$ if and only if $p_\beta(F^{-1}H) = 0$ for all $\beta \not\leq \alpha$. Using the Cauchy-Binet formula, we have

$$p_\beta(F^{-1}H) = \sum_{\gamma \in \binom{[n]}{k}} p_{\beta,\gamma}(F^{-1})p_\gamma(H),$$

where $p_{\beta,\gamma}(F^{-1}) := \det((F^{-1})_{\beta_i,\gamma_j})_{i,j=1}^k$ is the (β, γ) -th entry in the matrix $\wedge^k(F^{-1})$.

Proposition 1.2 (Efficient equations for $Y \cap X_\alpha F$). *Let \mathcal{Y} be Stiefel coordinates for $Y \subset \text{Gr}(k, n)$ and compute the Plücker vector $P(\mathcal{Y}) := (p_\beta(\mathcal{Y}) \mid \beta \in \binom{[n]}{k})$ for \mathcal{Y} . Compute the rectangular matrix $P(\alpha)(F^{-1}) := (p_{\beta,\gamma}(F^{-1}) \mid \beta \not\leq \alpha, \gamma \in \binom{[n]}{k})$. The entries in the matrix-vector product $P(\alpha)(F^{-1}) \cdot P(\mathcal{Y})$ cut out $\phi(\mathcal{Y}) \cap X_\alpha F$ from $\phi(\mathcal{Y})$.*

Remark 1.3. There are further improvements. If some Plücker coordinates vanish on \mathcal{Y} , then we do not compute them in the Plücker vector $P(\mathcal{Y})$ nor the corresponding columns of the matrix $P(\alpha)(F^{-1})$. Typically $P(\alpha)(F^{-1})$ is a constant matrix and is therefore inexpensive to compute. Also note that $P(\mathcal{Y})$ consists of minors of a matrix of variables and is therefore relatively expensive to compute. This method is even more relatively efficient for generating equations for the intersections of several Schubert varieties, as we need only compute $P(\mathcal{Y})$ once.

Remark 1.4. When this improvement was first implemented in software, it resulted in speedups of several to 60-fold. Computing the problem $(\alpha, \alpha, \alpha, \alpha)$ with six solutions, where $\alpha = (3, 4, 7, 8)$, previously took 20 minutes, but after this was implemented, it only took 20 seconds in our software [21].

1.4. Numerical homotopy continuation. The Littlewood-Richardson homotopy is a numerical homotopy continuation algorithm. This is a class of numerical algorithms that compute the solutions to a system of polynomial equations by following the (known) solutions to a different set of equations along a deformation (homotopy) between the two using predictor-corrector methods. We elaborate.

Suppose that we want to compute the solutions to a system

$$f_1(x_1, \dots, x_m) = f_2(x_1, \dots, x_m) = \dots = f_M(x_1, \dots, x_m) = 0 \quad (4)$$

of polynomial equations. A *homotopy* for (4) is a one parameter family of equations $H(x; t) = 0$ whose solutions at $t = 0$ are known and whose solutions at $t = 1$ include those of (4). Furthermore, restricting t to lie in the interval $[0, 1]$ defines paths in \mathbb{C}^m that connect the solutions of (4) at $t = 1$ to known solutions at $t = 0$.

Given such a homotopy, standard predictor-corrector methods (explained in [28] or in [1]) are used to numerically trace the known solutions at $t = 0$ to obtain solutions to (4) at $t = 1$. The homotopy is *optimal* if every solution at $t = 0$ is connected to a unique solution to (4) at $t = 1$ along a path.

This procedure may be iterated, connecting one homotopy to another to solve (4) from known solutions to another system in two or more steps. The Pieri homotopy was such an optimal homotopy that used up to $k(n-k)-2$ steps to solve special Schubert problems [16]. The Littlewood-Richardson homotopy is also an optimal homotopy.

2. LITTLEWOOD-RICHARDSON HOMOTOPY

The Littlewood-Richardson homotopy algorithm is based on the geometric Littlewood-Richardson rule [35]. This is a sequence of degenerations which successively transform an intersection $X_\alpha F \cap X_\beta M$ of Schubert varieties when F and M are general into a union of Schubert varieties $X_\gamma F$ where $\|\gamma\| = \|\alpha\| + \|\beta\|$. Given points in all the Schubert varieties $X_\gamma F$ that satisfy some equations, we may numerically follow these solutions backwards along the degenerations to obtain solutions to these equations in $X_\alpha F \cap X_\beta M$. **Refer to a result in Valik's paper.**

Given a Schubert problem β^1, \dots, β^s , suppose that we know all the points of

$$X_\gamma F \cap X_{\beta^3} F^3 \cap \dots \cap X_{\beta^s} F^s \quad (5)$$

for γ any index with $\|\gamma\| = \|\beta^1\| + \|\beta^2\|$. Then we may find all solutions to the instance of the Schubert problem

$$X_{\beta^1} F \cap X_{\beta^2} F^2 \cap X_{\beta^3} F^3 \cap \dots \cap X_{\beta^s} F^s \quad (6)$$

as follows. First, formulate membership in $X_{\beta^3} F^3 \cap \dots \cap X_{\beta^s} F^s$ as a system of polynomial equations. Then use the geometric Littlewood-Richardson rule for $X_{\beta^1} F \cap X_{\beta^2} F^2$ to follow the points of (5) for all γ back to solutions to the instance (6) of the original Schubert problem.

Consequently, if for some i we know all solutions to instances of Schubert problems of the form

$$X_\gamma F \cap X_{\beta^i} F^i \cap \dots \cap X_{\beta^s} F^s$$

for all γ , then we may find all solutions to Schubert problems of the form

$$X_\alpha F \cap X_{\beta^{i-1}} F^{i-1} \cap X_{\beta^i} F^i \cap \dots \cap X_{\beta^s} F^s.$$

Thus starting with the (known) solution (2) to $X_\gamma F \cap X_{\beta^s} F^s$, in $s-1$ iterations of this procedure we obtain all solutions to the original Schubert problem.

The geometry of these degenerations in the geometric Littlewood-Richardson rule is encoded in the combinatorial checkerboard game. **Reference?** We combine $s-1$ of these games into a checkerboard tournament that encodes the process of resolving a given Schubert problem. This forms the combinatorial backbone of the Littlewood-Richardson homotopy.

Subsection 2.1 defines Stiefel coordinates for the varieties which arise. Subsection 2.2 describes the combinatorial checkerboard game, and explains how these connect to get a checkerboard tournament. Subsection 2.3 is the most important. It describes in some detail how each step of a checkerboard game is translated into equations and a homotopy, and then how these are linked together in the Littlewood-Richardson homotopy. This is the mathematical core of the Littlewood-Richardson homotopy algorithm.

2.1. Checkerboard varieties. We summarize salient features of [35]. The geometric Littlewood-Richardson rule for a pair α, β of brackets is a sequence of $\binom{n}{2} + 1$ families of subvarieties parametrized by pairs of flags (F, M) in particular special positions. These families fit together pairwise into $\binom{n}{2}$ flat families[†]. The most general family is

[†]Find results in Vakil's papers to cite

parametrized by pairs (F, M) of flags in general position with the fiber over (F, M) the intersection of Schubert varieties $X_\alpha F \cap X_\beta M$, and the least general family is parametrized by flags F with fibers unions of Schubert varieties $X_\gamma F$ where $\|\gamma\| = \|\alpha\| + \|\beta\|$. This transforms the intersection of two Schubert varieties into a union of Schubert varieties.

These $\binom{n}{2}$ families have the same base for any two brackets α, β —each consists of all pairs (F, M) of flags having a particular relative position. The relative position of two flags F and M is encoded by a permutation π , where

$$\dim(M_i \cap F_j) = \#\{\ell \leq j \mid \pi(\ell) \leq i\}.$$

We encode this special position in a *permutation array*, which is an $n \times n$ array of boxes with the box in row $\pi(i)$ and column i occupied by a black checker, \bullet . We will refer to a permutation array by the corresponding permutation π .

The permutations occurring in the geometric Littlewood-Richardson rule are those in the bubble sort of the permutation ω_0 , where $\omega_0(i) = n+1-i$, which corresponds to two flags in general position. An ordered basis $\mathbf{m}_1, \dots, \mathbf{m}_n$ for \mathbb{C}^n and a permutation array π define flags F and M : Identifying the checker in row i with \mathbf{m}_i , so that $\mathbf{m}_{\pi(j)}$ is in column j , the i -plane M_i is the span of the checkers in the first i rows and the i -plane F_i is the span of the checkers in the first i columns.

The set of pairs of flags F, M with relative position π forms the base of a family of checkerboard varieties, which are themselves encoded by certain placements of k red checkers in the permutation array π . In these placements the red checkers are in distinct rows and columns, and any subset of j red checkers has at least j black checkers to its northwest (\nwarrow). Let $\bullet\bullet$ be such a placement and F, M be a flag given by an ordered basis $\mathbf{m}_1, \dots, \mathbf{m}_n$ where \mathbf{m}_i is identified with the black checker in row i . For each subset S of red checkers, let $S(F, M)$ be the subspace of \mathbb{C}^n spanned by the black checkers northwest of S . The *checkerboard variety* $Y_{\bullet\bullet}(F, M)$ consists of all k -planes H such that $\dim H \cap S(F, M) \geq \#S$, for all subsets S of red checkers.

The checkerboard variety $Y_{\bullet\bullet}(F, M)$ has Stiefel coordinates given by a ser $\mathcal{Y}_{\bullet\bullet}$ of matrices: Order the red checkers by row. The j th column of $\mathcal{Y}_{\bullet\bullet}$ has nonzero entries in the rows of the black checkers northwest of the j th checker with a 1 in the row of the j th checker. The set $\phi(M\mathcal{Y}_{\bullet\bullet})$ is dense in $Y_{\bullet\bullet}(F, M)$, so that $M\mathcal{Y}_{\bullet\bullet}$ is Stiefel coordinates for $Y_{\bullet\bullet}(F, M)$. A k -plane $H \in \phi(M\mathcal{Y}_{\bullet\bullet})$ has a basis $\mathbf{h}_1, \dots, \mathbf{h}_k$ where

$$\mathbf{h}_j = \sum_{i=1}^n y_{i,j} \mathbf{m}_i,$$

where $y_{i,j}$ is the entry in row i and column j of $\mathcal{Y}_{\bullet\bullet}$. That is,

$$\begin{aligned} y_{i,j} &= 0 && \text{unless the black checker in row } i \text{ is northwest of the } j\text{th red checker} \\ &= 1 && \text{if the } j\text{th red checker is in the row of the } i\text{th black checker,} \end{aligned}$$

and otherwise $y_{i,j}$ is an indeterminate.

Figure 1 shows a checkerboard and its associated coordinates when $n = 14$ and $k = 7$, and the underlying permutation is $\pi = (6, 7, 8, 9, 11, 12, 13, 14, 10, 5, 4, 3, 2, 1)$. The entries \cdot in the coordinate matrix are 0s. The capital letters A — F and arrows will be explained later.

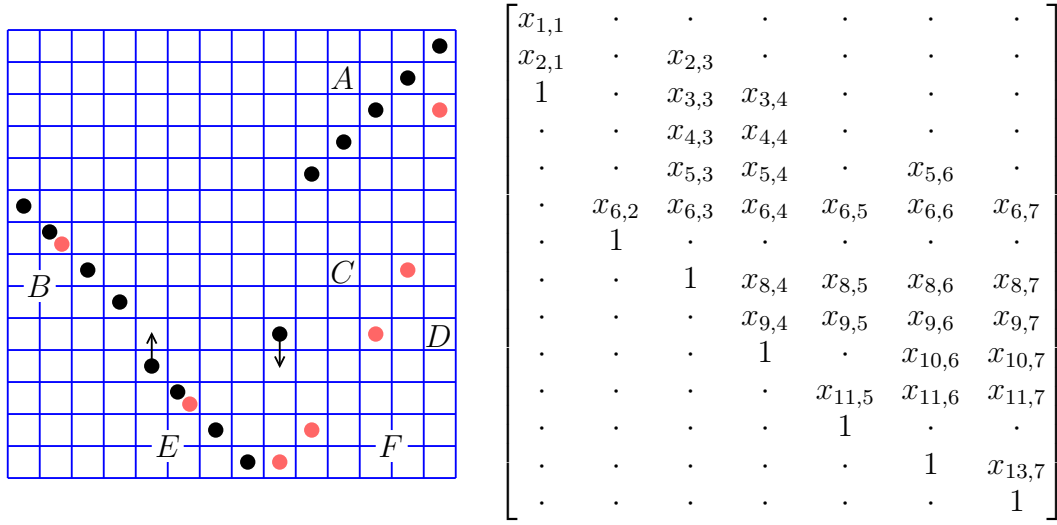


FIGURE 1. Stiefel coordinates corresponding to a checkerboard.

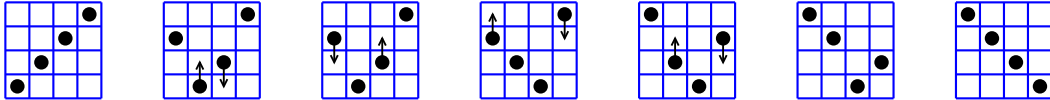
2.2. The checkerboard game. The steps in the geometric Littlewood-Richardson rule, the deformations and degenerations of $X_\alpha F \cap X_\beta M$ and of subsequent checkerboard varieties, are encoded in the combinatorial checkers game.

We first describe the movement of the black checkers, which begins with the permutation ω_0 where the black checkers are along the anti-diagonal in positions (i, j) with $i + j = n + 1$. In the checkerboard game, the black checkers remain in their respective columns, interchanging rows. The first move interchanges the lowest (leftmost) two checkers.

For subsequent moves, note that at a permutation σ in mid-sort, the black checkers will be in one of four regions: (A) the upper right portion of the anti-diagonal, (B) along a diagonal starting in the first column in the row below (A), (E) along a diagonal starting one column and two rows after (B), and there will be a single checker (D) in the column between (A) and (E) and in the row between (B) and (E). If there is no column between the checkers in (A) and those along a diagonal, then that diagonal is (E), (B) is empty, and the solitary checker is the last checker in (A). The solitary checker is the *descending checker* and the top checker in (E) is the *ascending checker*.

The subsequent permutation array π is obtained by interchanging the rows of the descending and ascending checkers. Call the row of the descending checker the *critical row* and the diagonal (E) the *critical diagonal*. See Figure 2.

When $n = 4$, there are $7 = \binom{4}{2} + 1$ permutation arrays in the bubble sort.



The checkerboard game constructs a tree with $\binom{n}{2} + 1$ levels whose nodes are checkerboards. Its root encodes the intersection $X_\alpha F \cap X_\beta M$ as a checkerboard as follows: On a board with black checkers along the antidiagonal, place red checkers in positions

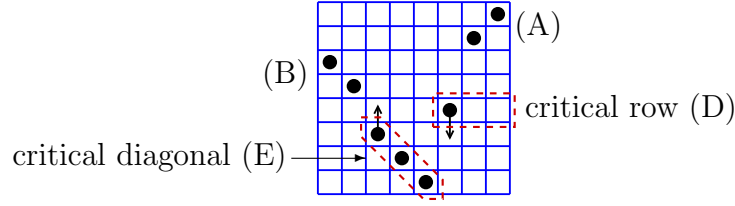
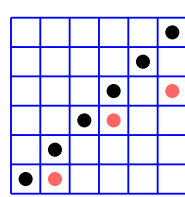


FIGURE 2. Critical row and critical diagonal.

$(\beta_{k+1-i}, \alpha_i)$ for $i = 1, \dots, k$. For example, when $n = 6$ and $k = 3$ with $\alpha = (2, 4, 6)$ and $\beta = (3, 4, 6)$, we have:



$$\begin{bmatrix} \cdot & \cdot & x_{13} \\ \cdot & \cdot & x_{23} \\ \cdot & x_{32} & 1 \\ \cdot & 1 & \cdot \\ x_{51} & \cdot & \cdot \\ 1 & \cdot & \cdot \end{bmatrix}.$$

If for some i , $\beta_{k+1-i} + \alpha_i < n$, then $X_\alpha F \cap X_\beta M = \emptyset$ and we do not have a checkerboard game in this case.

Each node in the checkerboard tree has one or two children according to which of nine cases it is in. These are determined by two questions, each of which has three answers.

Where is the top red checker in the critical diagonal?

- (0) In the rising checker's square.
- (1) Elsewhere in the critical diagonal.
- (2) There is no red checker in the critical diagonal.

Where is the red checker in the critical row?

- (0) In the descending checker's square.
- (1) Elsewhere in the critical row.
- (2) There is no red checker in the critical row.

Table 1 shows the movement of the checkers in these nine cases. The rows correspond to the answers to the first question and the columns to the answers of the second question. Only the relevant part of each checkerboard is shown.

In case (1, 1) there are two possibilities, which can both occur—this is when the node has two children. They are referred to in the sequel as stay or swap, for in one the red checkers remain in place, while in the other, they change columns, swapping the basis element corresponding to the descending black checker. The second of these (swap) only occurs if there are no other red checkers in the rectangle between the two, called *blockers*. Figure 3 shows a blocker.

For a permutation π let P_π be the space of pairs of flags (F, M) in relative position π . If σ and π are two permutations in the bubble sort with π subsequent to σ , then in the space of pairs of flags, P_π is a subset of the closure P_σ , and is a dense subset of a component of $\overline{P_\sigma} \setminus P_\sigma$ so that $\overline{P_\pi}$ is a boundary divisor of P_σ .

Suppose that $\bullet\bullet'$ is a checkerboard with permutation array σ and child checkerboard $\bullet\bullet$ with permutation array π (or $\bullet\bullet_{\text{stay}}$ and $\bullet\bullet_{\text{swap}}$ are its two children in case (1, 1)). Consider

	0	1	2
0			
1		or	
2			

TABLE 1. Movement of red checkers.

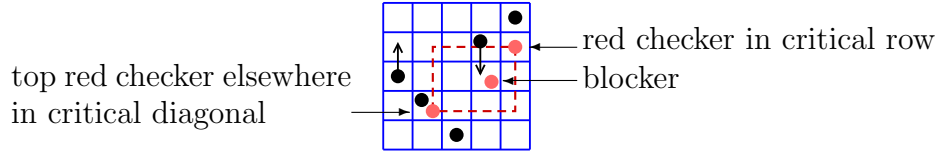


FIGURE 3. a blocker.

the space Y over $P_\sigma \cup P_\pi \subset \overline{P_\sigma}$ whose fiber over $(F, M) \in P_\sigma$ is the checkerboard variety $Y_{\bullet\bullet}(F, M)$ and over $(F, M) \in P_\pi$ is the checkerboard variety $Y_{\bullet\bullet}(F, M)$ (or $Y_{\bullet\bullet\text{stay}}(F, M) \cup Y_{\bullet\bullet\text{swap}}(F, M)$ in case (1,1)). Then Vakil's Theorem [35, Thm. ??] states that Y is a flat family and in fact Y is the closure in $(P_\sigma \cup P_\pi) \times \text{Gr}(k, n)$ of the restriction of Y to P_σ .

At the conclusion of the checkerboard game, the black checkers occupy the main diagonal and the red checkers lie along the main diagonal. Each checkerboard corresponds to the Schubert variety $X_\gamma F$, where the red checkers lie in positions $(\gamma_1, \gamma_1), \dots, (\gamma_k, \gamma_k)$.

Figure 4 shows this checkerboard game in the first nontrivial case when $n = 4$, $k = 2$ and $\alpha = \beta = (2, 4)$. The arrows are labeled by the position of the checkerboard move in

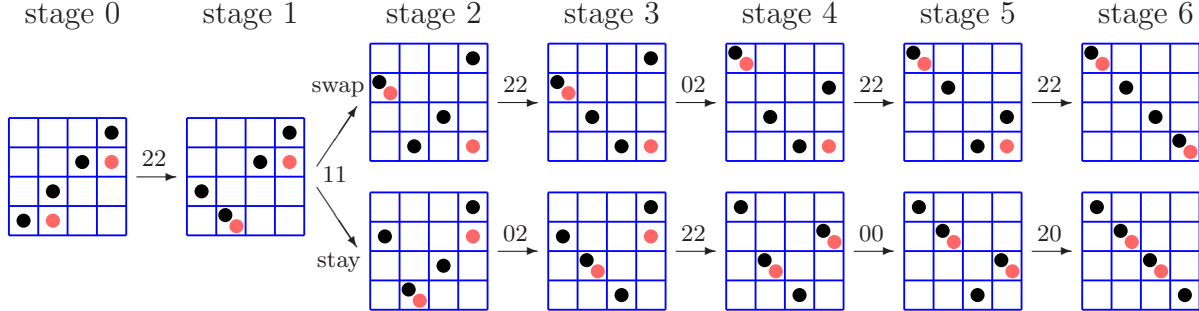
FIGURE 4. Resolving the intersection $X_{(2,4)}F \cap X_{(2,4)}M$.

Table 1.

This checkerboard tree may have identical nodes. Since the children of a node depend only on the checkerboard of that node, we may identify identical nodes, obtaining a ranked poset whose maximal elements (leaves) will be indexed by a subset of those γ with $\|\gamma\| = \|\alpha\| + \|\beta\|$.

Suppose that we have a Schubert problem, $(\beta^1, \beta^2, \dots, \beta^s)$. The checkerboard poset for β^1, β^2 will have leaves indexed by sequences α with $\|\alpha\| = \|\beta^1\| + \|\beta^2\|$. For each such α , we may form the checkerboard poset for α, β^3 , and attach it to the leaf labeled α . Identifying identical nodes in this new poset gives a poset whose leaves are indexed by γ with $\|\gamma\| = \|\beta^1\| + \|\beta^2\| + \|\beta^3\|$. Repeating this process forms the *checkerboard tournament*, which is a poset having $s-2$ levels of checkerboard posets, and whose leaves are labeled by sequences δ with $\|\delta\| + \|\beta^s\| = k(n-k)$. We may prune this poset, leaving only the single leaf labeled by the sequence $\delta = (n+1-\beta_k^s, \dots, n+1-\beta_1^s)$. Vakil's Theorem [Cite this properly](#) is that the number of solutions to the original Schubert problem is the number of saturated chains in this poset from the root to the unique leaf.

2.3. Explicit coordinates for checkerboard moves. To produce a homotopy algorithm from the geometric Littlewood-Richardson rule, we select $\binom{n}{2}+1$ pairs of flags (F, M) with relative positions π , one pair for each permutation in the bubble sort. We also select $\binom{n}{2}$ one-parameter families of pairs $(F'(t), M'(t))$ that connect these flags. For us, the flags F and $F(t)$ are fixed to be the standard coordinate flag, so we only need to specify the flags M and $M(t)$. These have the following property. If M' is the flag corresponding to a permutation σ and M corresponds to the next permutation π in the bubble sort, then the family $M'(t)$ connecting them satisfies

$$M'(0) = M \quad \text{and} \quad M'(1) = M', \quad (7)$$

and for almost all $t \neq 0$, the pair $(F, M'(t))$ has relative position σ .

As F is the standard coordinate flag, F_i is spanned by $\mathbf{e}_1, \dots, \mathbf{e}_i$ where \mathbf{e}_i is the i th column of the identity matrix. At a permutation π in the bubble sort the flag M is given by an ordered basis $\mathbf{m}_1, \dots, \mathbf{m}_n$ so that M_i is spanned by $\mathbf{m}_1, \dots, \mathbf{m}_i$ and the coordinate subspace F_i is spanned by $\mathbf{m}_{\pi(1)}, \dots, \mathbf{m}_{\pi(i)}$, but $\mathbf{m}_1, \dots, \mathbf{m}_n$ is not necessarily a permutation of $\mathbf{e}_1, \dots, \mathbf{e}_n$.

At the leaves of a checkerboard game we have that $M = F$, so that $\mathbf{m}_i = \mathbf{e}_i$ for $i = 1, \dots, n$. We describe the other flags recursively. Suppose that M is the flag corresponding to a permutation π in the bubble sort with σ the previous permutation, and let r be the critical row in the sort from σ to π . Then the flag M' corresponding to σ is given by the basis $\mathbf{m}'_1, \dots, \mathbf{m}'_n$, where

$$\mathbf{m}'_i = \mathbf{m}_i \quad \text{for } i \neq r, r+1, \quad \mathbf{m}'_r = \mathbf{m}_r - \mathbf{m}_{r+1}, \quad \text{and} \quad \mathbf{m}'_{r+1} = \mathbf{m}_r.$$

For $t \neq 0$, the family $M'(t)$ connecting these two flags is given by the basis $\mathbf{m}'_1(t), \dots, \mathbf{m}'_n(t)$, where

$$\begin{aligned} \mathbf{m}'_i(t) &= \mathbf{m}_i = \mathbf{m}'_i & i \neq r, r+1, \\ \mathbf{m}'_r(t) &= \mathbf{m}_r - t\mathbf{m}_{r+1} = t\mathbf{m}'_r + (1-t)\mathbf{m}'_{r+1}, & \text{and} \\ \mathbf{m}'_{r+1}(t) &= \mathbf{m}_r = \mathbf{m}'_{r+1}. \end{aligned}$$

When $t = 0$, set $M'(0) = M$ and note that $\lim_{t \rightarrow 0} M'(t) = M(0) = M$ and $\langle \mathbf{m}'_r(t), \mathbf{m}'_{r+1}(t) \rangle = \langle \mathbf{m}_r, \mathbf{m}_{r+1} \rangle$. The flag M at the root corresponds to the triangular matrix $(m_{i,j})$, where

$$m_{i,j} = \begin{cases} 0 & \text{if } n < j + i \\ (-1)^i & \text{otherwise} \end{cases}.$$

Figure 5 shows the permutations π , permutation arrays, matrices M , and families $M'(t)$ when $n = 4$.

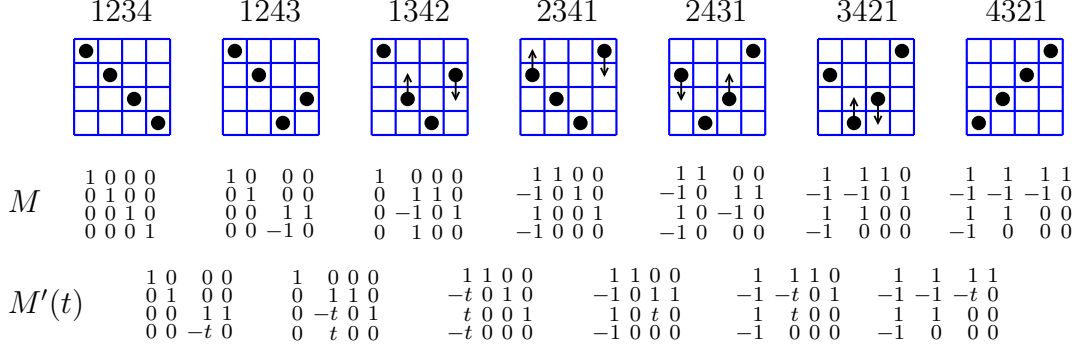


FIGURE 5. Permutation arrays, matrices M , and families of matrices $M(t)$.

Remark 2.1. In passing from the permutation π to the preceding permutation σ in the bubble sort (opposite to the arrows in the checkerboard game), the black checkers in rows r and $r+1$ switch rows,

$$\pi : \begin{array}{|c|c|c|c|} \hline \bullet & \dots & & \\ \hline & & & \bullet \\ \hline \end{array} \quad \text{becomes} \quad \sigma : \begin{array}{|c|c|c|c|} \hline & \dots & \bullet & \\ \hline \bullet & \dots & & \\ \hline \end{array}.$$

In passing from the flag M for π to the flag M' for σ , we have $\mathbf{m}'_{r+1} = \mathbf{m}_r$ and $\mathbf{m}'_r = \mathbf{m}_r - \mathbf{m}_{r+1}$. Thus the basis element corresponding to the left moving checker is unchanged, while that corresponding to the right checker is changed.

As there are ten different checkerboard moves in Table 1, there are potentially ten different families of coordinates for checkerboard varieties over the family of pairs $(F, M'(t))$. Analyzing their geometry reveals there are only three geometrically distinct cases, with the last subdivided into two further subcases. We indicate these cases by their positions in the 3×3 array of Table 1,

$$\text{I : } \begin{array}{|c|c|c|} \hline & & \text{x} \\ \hline & & \text{x} \\ \hline & & \text{x} \\ \hline \end{array}, \quad \text{II : } \begin{array}{|c|c|c|} \hline & & \\ \hline & \text{stay} & \\ \hline \text{x} & & \text{x} \\ \hline \end{array}, \quad \text{III(a) : } \begin{array}{|c|c|c|} \hline & & \\ \hline \text{x} & \text{swap} & \\ \hline & & \\ \hline \end{array}, \quad \text{and} \quad \text{III(b) : } \begin{array}{|c|c|c|} \hline \text{x} & \text{x} & \\ \hline & & \\ \hline & & \\ \hline \end{array},$$

and refer to them by the numerals I, II, III(a), and III(b) in the sequel.

2.3.1. Case I. When there is no red checker in the critical row (the third column of Table 1), the geometric condition on the k -plane does not change, as we can see by Remark 2.1. In this case, we only need to explain how to transform the coordinates $\mathcal{Y}_{\bullet\bullet}$ of a given k -plane into those of $\mathcal{Y}_{\bullet\bullet'}$ so that

$$M' \mathcal{Y}_{\bullet\bullet'} = M \mathcal{Y}_{\bullet\bullet}. \quad (8)$$

Let σ be the permutation underlying $\bullet\bullet'$ and π the permutation underlying $\bullet\bullet$. Write $y'_{i,j}$ for the entries of $\mathcal{Y}_{\bullet\bullet'}$ and $y_{i,j}$ for the entries of $\mathcal{Y}_{\bullet\bullet}$, and let r be the critical row. If we set

$$y'_{i,j} := y_{i,j} \quad i \neq r, r+1, \quad y'_{r,j} := -y_{r+1,j}, \quad \text{and} \quad y'_{r+1,j} := y_{r,j} + y_{r+1,j},$$

then (8) is satisfied.

If there is a red checker in row $r+1$ of $\bullet\bullet'$, then its column will not be in echelon form in $\mathcal{Y}_{\bullet\bullet}$: If its column index is j , then the last two entries are in rows r and $r+1$, and they are $y'_{r,j} = -1$ and $y'_{r+1,j} = 1 + y_{r,j}$. In this case, we simply divide that column by $y'_{r+1,j}$ to put $\mathcal{Y}_{\bullet\bullet}$ into echelon form.

2.3.2. Case II. Let $\bullet\bullet$ be the checkerboard position corresponding to π and $\bullet\bullet'$ that corresponding to σ . We define a family $\mathcal{Y}_{\bullet\bullet}(t)$ of matrices and show that $M\mathcal{Y}_{\bullet\bullet}(t)$ provides Stiefel coordinates for the checkerboard variety over $(F, M'(t))$. That is, $\phi M\mathcal{Y}_{\bullet\bullet}(0)$ is dense in $Y_{\bullet\bullet}(F, M)$ and $\phi M\mathcal{Y}_{\bullet\bullet}(t)$ is dense in $Y_{\bullet\bullet'}(F, M'(t))$ for $t \neq 0$.

Let $(y_{i,j})$ be the entries in the coordinates $\mathcal{Y}_{\bullet\bullet}$, as given at the end of Subsection 2.1. We set $\mathcal{Y}_{\bullet\bullet}(t) = (y_{i,j}(t))$, where $y_{i,j}(t) := y_{i,j}$, unless $i = r+1$ and checker j is not on the critical diagonal (see Figure 2). When j **does not lie** in the critical diagonal, we set

$$y_{r+1,j}(t) := y_{r+1,j} - ty_{r,j}.$$

We remark that if j lies in the critical diagonal, then $y_{r,j}$ is a non-zero indeterminate and $y_{r+1,j} = 0$, and the row of the j th checker is at least $r+2$. When checker j does not lie in the critical diagonal, but is in row r , then $y_{r,j} = 1$ and $y_{r+1,j} = 0$.

Lemma 2.2. *For any t , $\phi(M\mathcal{Y}_{\bullet\bullet}(t))$ is dense in the checkerboard variety over the pair $(F, M(t))$.*

Proof. When $t = 0$, this holds as $\mathcal{Y}_{\bullet\bullet}(0) = \mathcal{Y}_{\bullet\bullet}$, and we defined $\mathcal{Y}_{\bullet\bullet}$ so that $M\mathcal{Y}_{\bullet\bullet}$ gives Stiefel coordinates for $Y_{\bullet\bullet}(F, M)$, and $M'(0) = M$. For $t \neq 0$, we will show that $M'(t)\mathcal{Y}_{\bullet\bullet'} = M\mathcal{Y}_{\bullet\bullet}(t)$, by solving this equation for the entries of $\mathcal{Y}_{\bullet\bullet'}$, which will complete the proof.

The columns of $\mathcal{Y}_{\bullet\bullet}(t)$ correspond to vectors $\mathbf{h}_1(t), \dots, \mathbf{h}_k(t)$ in $M\mathcal{Y}_{\bullet\bullet}(t)$ that span the k -plane $\phi(M\mathcal{Y}_{\bullet\bullet}(t))$. If the j th checker lies on the critical diagonal, then

$$\mathbf{h}_j(t) = \sum_{i \neq r, r+1} y_{i,j} \mathbf{m}_i + y_{r,j} \mathbf{m}_r + 0 \cdot \mathbf{m}_{r+1},$$

and if the j th checker is not on the critical diagonal, then

$$\mathbf{h}_j(t) = \sum_{i \neq r, r+1} y_{i,j} \mathbf{m}_i + y_{r,j} \mathbf{m}_r + y_{r+1,j} \mathbf{m}_{r+1} - y_{r,j} t \mathbf{m}_r.$$

Recall that if $i \neq r, r+1$, $\mathbf{m}'_i(t) = \mathbf{m}_i$, and we have $\mathbf{m}'_{r+1}(t) = \mathbf{m}_r$, and $\mathbf{m}'_r(t) = \mathbf{m}_r - t\mathbf{m}_{r+1}$, so that when $t \neq 0$, we have

$$\mathbf{m}_{r+1} = \frac{1}{t}(\mathbf{m}'_{r+1}(t) - \mathbf{m}'_r(t)).$$

Then if j lies on the critical diagonal, we have

$$\mathbf{h}_j(t) = \sum_{i \neq r, r+1} y_{i,j} \mathbf{m}'_i(t) + y_{r,j} \mathbf{m}'_{r+1}(t),$$

and if the j th checker is not on the critical diagonal, then

$$\mathbf{h}_j(t) = \sum_{i \neq r, r+1} y_{i,j} \mathbf{m}'_i(t) + (y_{r,j} - \frac{1}{t} y_{r+1,j}) \mathbf{m}'_r(t) + \frac{1}{t} y_{r+1,j} \mathbf{m}'_{r+1}(t).$$

If we define $\mathcal{Y}_{\bullet\bullet'}(t) = (y'_{i,j}(t))$ for $t \neq 0$ by

$$y'_{i,j}(t) = y_{i,j} \quad \text{for } i \neq r, r+1,$$

and if j lies on the critical diagonal, then

$$y'_{r,j}(t) = 0 = y_{r+1,j} \quad \text{and} \quad y'_{r+1,j}(t) = y_{r,j},$$

and if j does not lie on the critical diagonal, then

$$y'_{r,j}(t) = y_{r,j} - \frac{1}{t} y_{r+1,j} \quad \text{and} \quad y'_{r+1,j}(t) = \frac{1}{t} y_{r+1,j},$$

then if $\mathbf{h}'_1(t), \dots, \mathbf{h}'_k(t)$ are the vectors from $M'(t)\mathcal{Y}_{\bullet\bullet'}(t)$ corresponding to the columns of $\mathcal{Y}(t)$, we have $\mathbf{h}'_j(t) = \mathbf{h}_j(t)$ for $t \neq 0$, which proves the lemma. **Run on Sentence!** \square

Remark 2.3. For the homotopy in this case, we use the $n \times k$ matrix $M\mathcal{Y}_{\bullet\bullet}(t)$ as Stiefel coordinates to generate equations for the points in $Y_{\bullet\bullet}(F, M'(t)) \cap Z$, where Z is the remaining Schubert conditions. This gives a homotopy between

$$Y_{\bullet\bullet}(F, M) \cap Z \quad \text{and} \quad Y_{\bullet\bullet'}(F, M') \cap Z$$

at $t = 0$ and $t = 1$. Given the solutions $\mathcal{Y}_{\bullet\bullet}(1) = (y_{i,j}(1))$ to this at $t = 1$, we transform these into the coordinates $\mathcal{Y}_{\bullet\bullet'}$:

$$\begin{aligned} y'_{i,j} &= y_{i,j}(t) & \text{for } i \neq r, r+1, \\ y'_{r,j} &= 0 & \text{and } y'_{r+1,j} = y_{r,j}(1) \quad j \in E, \quad \text{and} \\ y'_{r+1,j} &= y_{r+1,j}(1) & \text{and } y'_{r,j} = y_{r,j}(1) - y_{r+1,j}(1). \end{aligned}$$

2.3.3. Case III.

3. IMPLEMENTATION DETAILS

Probably a poor choice for section title, but this includes aspects of the algorithm not covered in the previous section. Particularly the distinction between the three levels coordinates used in the computation: internal (given by the moving flag), computer coordinates, and absolute (user) coordinates.

Changing flags between boards of a checkerboard tournament

Let $M = (m_{i,j})$ be the moving flag at the root of a checkerboard game, so that

$$m_{i,j} = \begin{cases} 0 & \text{if } n < j + i \\ (-1)^i & \text{otherwise} \end{cases}.$$

Then the Schubert problem corresponding to that root is

$$(\alpha^1, M), (\alpha^2, I_n), (\alpha^3, F'_3), \dots, (\alpha^s, F'_s).$$

(Note that the $n \times k$ matrix S of variables parametrizing the Richardson variety $X_{\alpha^1}M \cap X_{\alpha^2}I_n$ is presented as the usual local coordinates for $X_{\alpha^1}rI_n \cap X_{\alpha^2}I_n$ so that MS is the Stiefel coordinates for $X_{\alpha^1}M \cap X_{\alpha^2}I_n$, which is used in the equations for the remaining Schubert varieties in the Schubert problem.) This must be transformed into a Schubert problem for the corresponding leaf of the previous checkerboard, which is the Schubert problem

$$(\alpha^1, I_n), (\alpha^2, F_2), (\alpha^3, F_3), \dots, (\alpha^s, F_s).$$

We use a linear transformation to effect this coordinate change. First, we solve the equations

$$AM = I_n T_1 \quad \text{and} \quad AI_n = F_2 T_1,$$

where A is a square matrix and T_1, T_2 are upper triangular matrices (so that I_n and T_1 give the same flag, as do F_2 and $F_2 T_2$). Then, we set $F'_i := AF_i$ for $i = 3, \dots, s$.

It follows that to transfer a solution S to $(*)$ to a solution to $(**)$, we simply compute AMS , but then we must column reduce this with respect to given pivots **Which we must describe**.

4. PERFORMANCE OF IMPLEMENTATION

This would discuss what can be computed, and will be the only place where we say anything more than in passing about the two implementations.

We will write a separate paper on this software for the Macaulay 2 Journal.

REFERENCES

1. Daniel J. Bates, Jonathan D. Hauenstein, Andrew J. Sommese, and Charles W. Wampler, *Numerically Solving Polynomial Systems with Bertini*, SIAM, 2103.
2. Guy Bresler, Dustin Cartwright, and David Tse, *Interference alignment for the mimo interference channel*, IEEE Trans on Info Theory., September 2014, [arXiv.org:1303.5678](https://arxiv.org/abs/1303.5678).
3. R. Brockett and C. Byrnes, *Multivariable Nyquist criteria, root loci, and pole placement: A geometric viewpoint*, Automatic Control, IEEE Transactions on **26** (1981), no. 1, 271–284.
4. C. I. Byrnes, *Pole assignment by output feedback*, Three Decades of Mathematical Systems Theory (H. Nijmeijer and J. M. Schumacher, eds.), Lecture Notes in Control and Inform. Sci., vol. 135, Springer-Verlag, Berlin, 1989, pp. 31–78.

5. C.I. Byrnes and P.K. Stevens, *Global properties of the root-locus map*, Feedback Control of Linear and Non-Linear Systems (D. Hinrichsen and A. Isidori, eds.), Lecture Notes in Control and Inform. Sci., vol. 39, Springer-Verlag, Berlin, 1982.
6. A. Eremenko and A. Gabrielov, *Pole placement by static output feedback for generic linear systems*, SIAM Journal on Control and Optimization **41** (2002), no. 1, 303–312.
7. W. Fulton, *Young tableaux*, London Mathematical Society Student Texts, vol. 35, Cambridge University Press, Cambridge, 1997.
8. L.D. García-Puente, N. Hein, C. Hillar, A. Martín del Campo, J. Ruffo, F. Sottile, and Z. Teitler, *The Secant conjecture in the real Schubert calculus*, Experimental Mathematics **21** (2012), no. 3, 252–265.
9. D.R. Grayson and M.E. Stillman, *Macaulay2, a software system for research in algebraic geometry*, Available at <http://www.math.uiuc.edu/Macaulay2/>.
10. J. Hauenstein, N. Hein, and F. Sottile, *A primal-dual formulation for certifiable computations in Schubert calculus*, Found. Comput. Math., to appear, 2015.
11. Jonathan D. Hauenstein, Andrew J. Sommese, and Charles W. Wampler, *Regeneration homotopies for solving systems of polynomials*, Math. Comp. **80** (2011), no. 273, 345–377.
12. N. Hein, C. Hillar, A. Martín del Campo, F. Sottile, and Z. Teitler, *The monotone secant conjecture in the real Schubert calculus*, Experimental Mathematics (2014).
13. N. Hein, C. Hillar, and F. Sottile, *Lower bounds in real schubert calculus*, São Paulo Journal of Mathematics **7** (2013), no. 1, 33–58.
14. N. Hein and F. Sottile, *A lifted square formulation for ceritifiable Schubert calculus*, [arXiv.org/1504.00979](https://arxiv.org/abs/1504.00979), 2015.
15. C. Hillar, L. García-Puente, A. Martín del Campo, J. Ruffo, Z. Teitler, S. L. Johnson, and F. Sottile, *Experimentation at the frontiers of reality in Schubert calculus*, Gems in Experimental Mathematics, Contemporary Mathematics, vol. 517, Amer. Math. Soc., Providence, RI, 2010, pp. 365–380.
16. B. Huber, F. Sottile, and B. Sturmfels, *Numerical schubert calculus*, Journal of Symbolic Computation **26** (1998), no. 6, 767 – 788.
17. B. Huber and B. Sturmfels, *A polyhedral method for solving sparse polynomial systems*, Math. Comp. **64** (1995), no. 212, 1541–1555.
18. B. Huber and J. Verschelde, *Pieri homotopies for problems in enumerative geometry applied to pole placement in linear systems control*, SIAM Journal on Control and Optimization **38** (2000), no. 4, 1265–1287.
19. S.L. Kleiman, *The transversality of a general translate*, Compositio Math. **28** (1974), 287–297.
20. S.L. Kleiman and D. Laksov, *Schubert calculus*, Amer. Math. Monthly **79** (1972), no. 10, 1061–1082.
21. Anton Leykin, Abraham Martín del Campo, Frank Sottile, Ravi Vakil, and Jan Verschelde, *Numericalschubertcalculus, a macaulay2 package for numerical computation in schubert calculus*, ??????, 2015.
22. Anton Leykin and F. Sottile, *Galois groups of Schubert problems via homotopy computation*, Math. Comp. **78** (2009), no. 267, 1749–1765.
23. T. Y. Li, Xiaoshen Wang, and Mengnien Wu, *Numerical Schubert calculus by the Pieri homotopy algorithm*, SIAM J. Numer. Anal. **40** (2002), no. 2, 578–600 (electronic).
24. A. Martín del Campo and F. Sottile, *Experimentation in the Schubert calculus*, Schubert Calculus — Osaka 2012 (H. Naruse, T. Ikeda, M. Masuda, and T. Tanisaki, eds.), Advanced Studies in Pure Mathematics, Mathematical Society of Japan, 2016.
25. M.S. Ravi, J. Rosenthal, and X. Wang, *Dynamic pole assignment and schubert calculus*, SIAM J. Control and Optim **34** (1996), 813–832.
26. J. Rosenthal and F. Sottile, *Some remarks on real and complex output feedback*, Systems Control Lett. **33** (1998), no. 2, 73–80.
27. J. Ruffo, Y. Sivan, E. Soprunova, and F. Sottile, *Experimentation and conjectures in the real Schubert calculus for flag manifolds*, Experiment. Math. **15** (2006), no. 2, 199–221.
28. A.J. Sommese and C.W. Wampler, II, *The numerical solution of systems of polynomials arising in engineering and science*, World Scientific Publishing Co. Pte. Ltd., Hackensack, NJ, 2005.

29. F. Sottile, *Pieri's formula via explicit rational equivalence*, *Canad. J. Math.* **49** (1997), no. 6, 1281–1298.
30. ———, *Real Schubert calculus: polynomial systems and a conjecture of Shapiro and Shapiro*, *Experiment. Math.* **9** (2000), no. 2, 161–182.
31. ———, *Enumerative real algebraic geometry*, *Algorithmic and quantitative real algebraic geometry* (Piscataway, NJ, 2001), DIMACS Ser. Discrete Math. Theoret. Comput. Sci., vol. 60, Amer. Math. Soc., Providence, RI, 2003, pp. 139–179.
32. ———, *Frontiers of reality in Schubert calculus*, *Bull. Amer. Math. Soc. (N.S.)* **47** (2010), no. 1, 31–71.
33. F. Sottile, R. Vakil, and J. Verschelde, *Solving Schubert problems with Littlewood-Richardson homotopies*, ISSAC 2010—Proceedings of the 2010 International Symposium on Symbolic and Algebraic Computation, ACM, New York, 2010, pp. 179–186.
34. F. Sottile and J. White, *Double transitivity of galois groups in the schubert calculus on grassmannians*, 2015, *Algebraic Geometry*, to appear.
35. R. Vakil, *A geometric Littlewood-Richardson rule*, *Ann. of Math. (2)* **164** (2006), no. 2, 371–421, Appendix A written with A. Knutson.
36. ———, *Schubert induction*, *Ann. of Math. (2)* **164** (2006), no. 2, 489–512.
37. J. Verschelde, *Algorithm 795: Phcpack: A general-purpose solver for polynomial systems by homotopy continuation*, *ACM Transactions on Mathematical Software* **25** (1999), no. 2, 251–276.
38. ———, *Numerical evidence for a conjecture in real algebraic geometry*, *Experiment. Math.* **9** (2000), no. 2, 183–196.
39. J. Verschelde and Y. Wang, *Computing dynamic output feedback laws*, *Automatic Control, IEEE Transactions on* **49** (2004), no. 8, 1393–1397.
40. ———, *Computing feedback laws for linear systems with a parallel pieri homotopy*, *Proceedings of the 2004 International Conference on Parallel Processing Workshops, ICCPW '04*, 2004, pp. 222–229.

SCHOOL OF MATHEMATICS, GEORGIA INSTITUTE OF TECHNOLOGY, 686 CHERRY STREET, ATLANTA, GA 30332-0160, USA

E-mail address: leykin@math.gatech.edu

URL: <http://people.math.gatech.edu/~aleykin3/>

ABRAHAM MARTÍN DEL CAMPO, CENTRO DE INVESTIGACIÓN EN MATEMÁTICAS, A.C., JALISCO S/N, COL. VALENCIANA, GUANAJUATO, GTO. MEXICO

E-mail address: abraham.mc@cimat.mx

URL: <http://personal.cimat.mx:8181/~abraham.mc/Home.html>

FRANK SOTTILE, DEPARTMENT OF MATHEMATICS, TEXAS A&M UNIVERSITY, COLLEGE STATION, TEXAS 77843, USA

E-mail address: sottile@math.tamu.edu

URL: www.math.tamu.edu/~sottile

RAVI VAKIL, DEPARTMENT OF MATHEMATICS, STANFORD UNIVERSITY, STANFORD, CA 94305 USA

E-mail address: vakil@math.stanford.edu

URL: <http://math.stanford.edu/~vakil>

JAN VERSCHELDE, DEPT OF MATH, STAT, AND CS, UNIVERSITY OF ILLINOIS AT CHICAGO, 851 SOUTH MORGAN (M/C 249), CHICAGO, IL 60607 USA

E-mail address: jan@math.uic.edu

URL: <http://www.math.uic.edu/~jan>